

Weak lensing probe of cubic Galileon model

Bikash R. Dinda,^{a,1}

^aCentre for Theoretical Physics, Jamia Millia Islamia,
New Delhi-110025, India

E-mail: bikash@ctp-jamia.res.in

Abstract. The cubic Galileon model containing the lowest non-trivial order action of the full Galileon action can produce the stable late-time cosmic acceleration. This model can have a significant role in the growth of structures. The signatures of the cubic Galileon model in the structure formation can be probed by the weak lensing statistics. Weak lensing convergence statistics is one of the strongest probes to the structure formation and hence it can probe the dark energy or modified theories of gravity models. In this work, we investigate the detectability of the cubic Galileon model from the Λ CDM model or from the canonical quintessence model through the convergence power spectrum and bi-spectrum.

¹Corresponding author.

Contents

1	Introduction	1
2	Action of the model	3
3	Background evolution	3
3.1	Initial conditions	5
3.2	Behaviour of some background quantities	5
4	Evolution of perturbations	7
4.1	Matter power spectrum	9
4.2	Matter bi-spectrum	11
5	Weak lensing statistics	13
5.1	Convergence power spectrum	14
5.2	Convergence bi-spectrum	15
6	Conclusion	17

1 Introduction

In literature, it is a well-known fact that the Universe is accelerating. This accelerating phase of the Universe is called late-time cosmic acceleration. Some observations like Supernova Type-Ia observations [1, 2], cosmic microwave background observations [3–5], baryon acoustic oscillations measurements [6, 7] confirm this fact. This acceleration can be explained by introducing an exotic matter called dark energy, which has negative pressure. The best possible simple dark energy model is the Λ CDM model. In this model at late time the Universe consists of cosmological constant, Λ (appx. 70% at present) and cold dark matter (CDM) component (appx. 30% at present) [5]. However, the Λ CDM model has some serious theoretical problem like the fine-tuning problem and cosmic coincidence problem [9]. Despite these theoretical problems, although it is the best possible fit to the most of the cosmological observations, recently some observations [10–13] suggest that it also has some inconsistencies to fit some data. This fact motivates us to go beyond the Λ CDM model. Another alternative to explain the cosmic acceleration is the dark energy with evolving equation of state such as quintessence [14–21] etc. Although very few evolving dark energy models like tracker models [14, 15] can be free from the cosmic coincidence problem, the fine-tuning problem is not avoidable.

Another popular alternative to the dark energy models is the modified theory of gravity [22–26], which can explain the late time cosmic acceleration. One of the modified theories of gravity is the Galileon gravity [27–36, 44–50]. The Galileon theory is obtained by taking the decoupling limit of the Dvali-Gabadadze-Porrati (DGP) [52]. In Galileon theory modification to the general relativity arises through a Galileon invariant scalar field, called Galileon. It is invariant under the Galileon shift symmetry $\partial_\mu\phi \rightarrow \partial_\mu\phi + b_\mu$ in 4-D Minkowski spacetime where b_μ is a constant vector. This Galileon shift symmetry confirms that the equation of motion remains second order in field derivatives despite the presence of the higher derivative

terms in the action [27, 45, 50] and the Galileon theory is free from Ostrogradsky ghosts [53]. The Galileon theory is a subset of the general Horndeski theory [54]. Although the shift symmetry breaks down in general cosmological metric like Friedmann-Robertson-Walker (FRW) metric, the equation of motion still remains second order by adding suitable couplings between Galileon derivatives and curvature tensors. Introduction of these types of coupling terms makes the modification to the general relativity highly non-trivial.

Due to the presence of such non-trivial terms, the modified theories of gravity possess the extra degree(s) of freedom which can affect the local physics which is extremely consistent with the general theory of relativity [55]. This extra degree of freedom is responsible for the 'fifth force'. This fifth force should be highly suppressed on the local scale such as in solar system as because on the local scale any modification to the Einstein's general theory of relativity is highly constrained [55]. The Vainshtein mechanism [56] is one of the mass screening methods which preserve the local physics in the modified theories of gravity models by suppressing the fifth force on local scales. In 1972 Vainshtein invented this method to address the van Dam-Veltman-Zakharov (vDVZ) discontinuity [57, 58] in the linear theory of massive gravity of Pauli-Fierz [59]. In general the Galileon gravity action contains five terms denoted by L_1 to L_5 . The Vainshtein mechanism is based on the term like $L_3 = (\partial_\mu \phi)^2 \square \phi$ [43, 51]. This is the lowest non-trivial term required for the mass screening in Vainshtein mechanism. L_4 term can take part in the mass screening but does not introduce any new physics [43]. L_5 term does not contribute to the mass screening [43]. In this paper, we consider up to the third terms. In literature generally, this is called cubic Galileon model. The second term is the usual canonical kinetic term. The second and third terms together only cannot give stable late time acceleration [46]. In addition to the second and third terms, the first term which is linear in Galileon field can produce stable acceleration. So, in Galileon theory the cubic Galileon model has the lowest non-trivial action which can produce stable late-time cosmic acceleration [37–43].

One of the major goals of the recent and upcoming high precision cosmological observations is to determine whether the late time cosmic acceleration is due to the Λ CDM model or any evolving dark energy model or any modified theory of gravity by studying the signatures of these models on both the background evolution of the Universe and the growth of the structures. Among these weak lensing experiments [69–82] are particularly promising to determine the nature of dark energy. In this paper, we address the prospect of probing cubic Galileon model in light of the weak lensing measurements by convergence statistics. Weak lensing is the statistical measure of the image distortion effect of the distant background galaxies due to gravitational bending of light by the intervening large scale structures along the photon geodesic. The weak lensing around massive halos was first measured in the nineties [60, 61] but the first measurement of weak lensing due to large scale structures was done independently by four groups in 2000 [62–65]. After that weak lensing become one of the strongest probes to the large scale structure formation. The main advantage of the weak lensing is that it solely depends on the underlying total matter-energy overdensity and hence complicated bias modeling can be avoided. Present and upcoming surveys like DES [66], LSST [67], Euclid [68], WFIRST etc. can provide us accurate weak lensing measurements which in turn can give us an accurate idea whether the late time cosmic acceleration is due to the Λ CDM model or any evolving dark energy model or any modified theory of gravity model.

Keeping these facts in mind, in this paper we aim to detect the signatures of the cubic Galileon model from the Λ CDM model or from the quintessence models using weak lensing statistics. We work in the unit, $C = \hbar = 1$ and we consider $(-, +, +, +)$ signature throughout

the paper.

The paper is organised as: in section 2 we briefly discuss the action of the cubic Galileon model; in section 3 background evolution has been studied; in section 4 we discuss the evolution of the perturbation in the cubic Galileon model; in section 5 we present the signature of the cubic Galileon model on the convergence power spectrum and bi-spectrum; and finally, in section 6 we present our conclusion.

2 Action of the model

We consider cubic Galileon model to study the evolutionary history of the Universe. The action for the cubic Galileon field, ϕ is given by [37–43]

$$S = \int d^4x \sqrt{-g} \left[\frac{M_{\text{pl}}^2}{2} R + \frac{1}{2} \sum_{i=1}^3 c_i \mathcal{L}_i \right] + \mathcal{S}_m, \quad (2.1)$$

where $\mathcal{L}_1 = M^3 \phi$, $\mathcal{L}_2 = (\nabla \phi)^2$ and $\mathcal{L}_3 = \frac{(\nabla \phi)^2}{M^3} \square \phi$. \mathcal{S}_m is the action for the matter counterpart, M_{pl} is the reduced Planck mass, M is a mass dimensional constant, c_i 's are dimensionless constants and g is the determinant of the metric describing the Universe. Note that full Galileon model has other two terms containing higher order derivatives of the Galileon field [44–49]. Those two terms involve nonminimal coupling. But cubic Galileon model considered here has no non-minimal coupling.

Note that for the matter counterpart we take cold dark matter (CDM) and baryons together as the total matter. For simplicity we take $c_2 = -1$ and this choice does not change the essence of the cubic galileon model. We define $\frac{c_3}{M^3} = -\frac{\alpha}{M^3} = -\beta$. Now we define the linear term in the action (2.1) in a way that it looks like a potential given by $V(\phi) = -\frac{1}{2}c_1 M^3 \phi$. So, the action (2.1) looks like [40–43]

$$S = \int d^4x \sqrt{-g} \left[\frac{M_{\text{pl}}^2}{2} R - \frac{1}{2} (\nabla \phi)^2 (1 + \beta \square \phi) - V(\phi) \right] + \mathcal{S}_m, \quad (2.2)$$

The purpose to write down the action (2.1) in the form given in equation (2.2) is that for $\beta = 0$ the action reduces to the standard quintessence action with linear potential [16–20].

3 Background evolution

For the background evolution of the Universe, we consider flat FRW metric given by $ds^2 = -dt^2 + a^2(t)d\vec{r} \cdot d\vec{r}$ where t is the cosmic time, \vec{r} is the comoving coordinate vector and a is the cosmic scale factor. Varying the action (2.2) with respect to the metric the background Einstein equations become [37–41]

$$3M_{\text{pl}}^2 H^2 = \bar{\rho}_{\text{m}} + \frac{\dot{\phi}^2}{2} (1 - 6\beta H \dot{\phi}) + V(\phi), \quad (3.1)$$

$$M_{\text{pl}}^2 (2\dot{H} + 3H^2) = -\frac{\dot{\phi}^2}{2} (1 + 2\beta \ddot{\phi}) + V(\phi), \quad (3.2)$$

where overdot is the derivative with respect to the cosmic time t , H is the Hubble parameter and $\bar{\rho}_{\text{m}}$ is the background matter energy density. The background Euler-Lagrangian equation for the Galileon field ϕ is given by [37–41]

$$\ddot{\phi} + 3H\dot{\phi} - 3\beta\dot{\phi}\left(3H^2\dot{\phi} + \dot{H}\dot{\phi} + 2H\ddot{\phi}\right) + V_\phi = 0, \quad (3.3)$$

where subscript ϕ is the derivative with respect to the field ϕ . Note that for the simplicity of the notation we take same ϕ as the background field.

To study the background evolution, in literature, it is a common practice to rewrite the above differential equations with an autonomous system of equations. To do so first we define some dimensionless background quantities given by [40, 41]

$$\begin{aligned} x &= \frac{\dot{\phi}}{\sqrt{6}HM_{Pl}} = \frac{\left(\frac{d\phi}{dN}\right)}{\sqrt{6}M_{Pl}}, & y &= \frac{\sqrt{V}}{\sqrt{3}HM_{Pl}}, \\ \epsilon &= -6\beta H\dot{\phi} = -6\beta H^2\left(\frac{d\phi}{dN}\right), & \lambda &= -M_{Pl}\frac{V_\phi}{V}, \\ \Gamma &= V\frac{V_{\phi\phi}}{V_\phi^2} = 0 \quad (\text{Here}), \end{aligned} \quad (3.4)$$

where $N = \ln a$ is the e-folding. Note that the quantity x here is different from the coordinate x used in eq. (2.1). In the subsequent sections by x we mean the quantity defined in Eq. (3.4). Using these quantities the autonomous system of equations become [40, 41]

$$\begin{aligned} \frac{dx}{dN} &= \frac{3x^3(2 + 5\epsilon + \epsilon^2) - 3x(2 - \epsilon + y^2(2 + 3\epsilon)) + 2\sqrt{6}y^2\lambda - \sqrt{6}x^2y^2\epsilon\lambda}{4 + 4\epsilon + x^2\epsilon^2}, \\ \frac{dy}{dN} &= -\frac{y(12(-1 + y^2)(1 + \epsilon) - 6x^2(2 + 4\epsilon + \epsilon^2) + \sqrt{6}x^3\epsilon^2\lambda + 2\sqrt{6}x(2 + (2 + y^2)\epsilon)\lambda)}{8 + 8\epsilon + 2x^2\epsilon^2}, \\ \frac{d\epsilon}{dN} &= -\frac{\epsilon(-3x(-3 + y^2)(2 + \epsilon) + 3x^3(2 + 3\epsilon + \epsilon^2) - 2\sqrt{6}y^2\lambda - \sqrt{6}x^2y^2\epsilon\lambda)}{x(4 + 4\epsilon + x^2\epsilon^2)}, \\ \frac{d\lambda}{dN} &= \sqrt{6}x\lambda^2(1 - \Gamma), \end{aligned} \quad (3.5)$$

where we have changed the time derivative to the derivative with respect to N . By using proper initial conditions (which are discussed in the next subsection), we solve the above-mentioned autonomous system of coupled differential equations to find the evolution of the background quantities.

Now, having solutions of the autonomous system of equations in Eq. (3.5) and from the above-mentioned dimensionless quantities in (3.4), we get some important background quantities given below: [40, 41]

$$\begin{aligned} \omega_\phi &= \frac{3x^2(\epsilon(\epsilon + 8) + 4) - 2\sqrt{6}\lambda xy^2\epsilon - 12y^2(\epsilon + 1)}{3(\epsilon(x^2\epsilon + 4) + 4)(x^2(\epsilon + 1) + y^2)}, \\ \Omega_\phi &= x^2(\epsilon + 1) + y^2, \\ \Omega_m &= 1 - \Omega_\phi, \\ H^2 &= H_0^2 \frac{\Omega_m^{(0)}(1 + z)^3}{\Omega_m}, \end{aligned} \quad (3.6)$$

where w_ϕ is the equation of state of the Galileon field, Ω_ϕ and Ω_m are the energy density parameters of the Galileon field and total matter respectively, H is the Hubble parameter, H_0 and $\Omega_m^{(0)}$ are the present day Hubble and matter-energy density parameters respectively and z is the redshift.

3.1 Initial conditions

First of all we fix the initial conditions of all the four quantities (x, y, ϵ and λ in Eq. (3.5)) at redshift $z = 1100$ in early matter-dominated era. At this redshift, we can neglect any contribution from the dark energy. In literature, we generally consider two types of initial conditions for these types of cosmological models. One is the tracker condition [14, 15] and another is the thawing condition [16–21]. In tracker models, the scalar field tracks the background initially and at late times the equation of state of the scalar field freezes to a constant value near to -1 . In thawing class of models, the scalar field is initially frozen to a value $w_\phi \approx -1$ due to the large Hubble friction in the early matter-dominated era. At late times the scalar field thaws away from its initial frozen state and the equation of state of the scalar field goes to higher values ($w_\phi > -1$) accordingly. It is a standard result we know that for linear potential tracker type of initial conditions is not possible accurately but the thawing class of initial conditions is perfectly possible. So, in our analysis we consider thawing class of initial conditions to solve the autonomous system of equations in Eq. (3.5).

In the thawing class of initial conditions Galileon field has $w_\phi \approx -1$ initially. It is possible for $x \ll 1$ which we can see through first line of Eq. (3.6); at $x \ll 1$, $w_\phi \approx \frac{-12y^2(\epsilon+1)}{3(4\epsilon+4)y^2} = -1$. So, we take $x_i = 10^{-8}$. The subscript 'i' refers to the initial value of any quantity at $z = 1100$. Note that the evolution of the background quantities is independent of x_i as long as $x_i \ll 1$.

The initial condition in y can be transferred to the boundary condition in Ω_ϕ through second line of Eq. (3.6). So, we find y_i by solving back $\Omega_\phi^{(0)} = 0.7$.

The initial value of λ controls the initial slopes of the potential. For $\lambda_i \ll 1$ the equation of state of the Galileon field does not deviate much from its initial value -1 i.e. it always stays very close to the cosmological constant behavior. For higher values of λ_i , the Galileon field sufficiently thaws away from the cosmological constant behavior accordingly. We consider $\lambda_i = 0.7$ for all the models.

Finally, we keep the initial condition in ϵ as a free parameter. So, we have only one free parameter (ϵ_i) in our case for the cubic Galileon model. Note that if we fix $\epsilon_i = 0$, the value of ϵ remains zero for the entire background evolution. So, the canonical quintessence model with linear potential is represented here by $c_3 = \alpha = \beta = \epsilon_i = \epsilon = 0$.

3.2 Behaviour of some background quantities

Before proceeding to the study of perturbation or structure formation, let us discuss some important background quantities.

In Fig. 1 we have plotted equation of state of the Galileon field. At sufficiently early time all the Galileon models have $w_\phi = -1$ and as time increases w_ϕ increases towards non-phantom values. $\epsilon_i = 0$ model has the highest deviation from the Λ CDM model in the non-phantom side. The value of w_ϕ decreases with increasing ϵ_i . However, the value of w_ϕ never goes to the phantom side. In the limiting end i.e. at $\epsilon_i \rightarrow \infty$ it approaches the Λ CDM value. So, the cubic Galileon model has always non-phantom behaviour.

In Fig. 2 we have shown $\Omega_\phi(z)$ vs. z plots. The right panel is the zoomed in version of the left panel for the redshift range 0.3 to 0.4. The horizontal green-dashed line has been

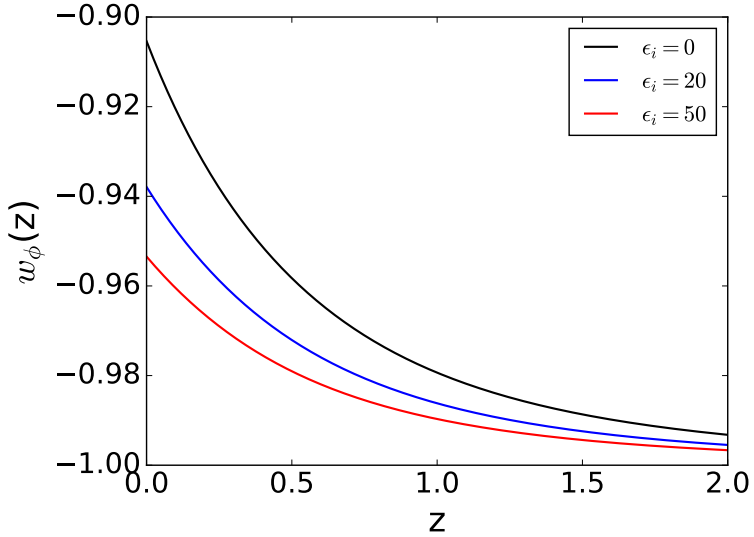


Figure 1. $w_\phi(z)$ vs. z plots.

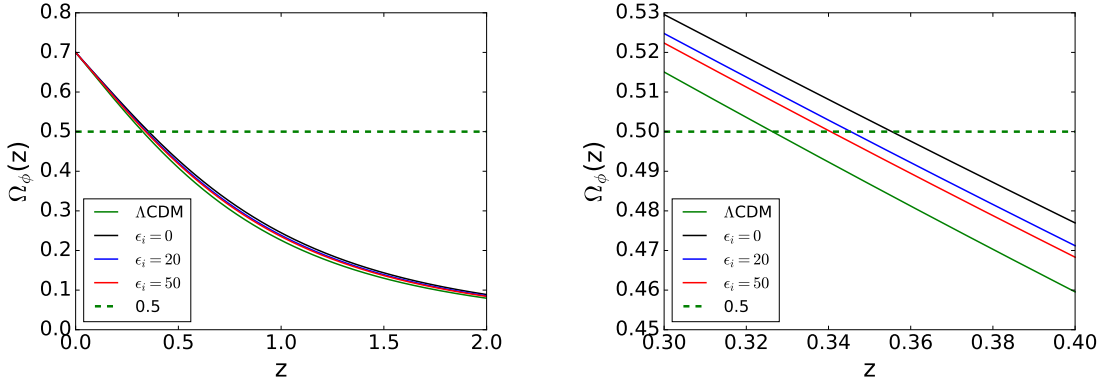


Figure 2. $\Omega_\phi(z)$ vs. z plots.

drawn at 0.5 to show at which redshift the Galileon field starts to dominate over total matter. In the $\epsilon_i = 0$ model, the Galileon field dominates earliest over the matter components. Larger the ϵ_i value later the domination of the Galileon field over matter.

In Fig. 3, we have plotted the deviations in the Hubble parameter from the Λ CDM model. Earlier the domination of the Galileon field over matter corresponds to the earlier domination of the accelerated phase of the expansion of the Universe. So, expansion of the scale factor relatively increases if the Galileon field dominates earlier. Since smaller ϵ_i value corresponds to the earlier domination of the Galileon field, the $\epsilon_i = 0$ model has the maximum positive deviation in the Hubble parameter from the Λ CDM model. Larger the ϵ_i value lower the deviation in the Hubble parameter. Since the cubic Galileon model always dominates earlier compared to the Λ CDM model irrespective to the value of ϵ_i (in the other way it is always non-phantom), the value of the Hubble parameter in cubic Galileon model is always

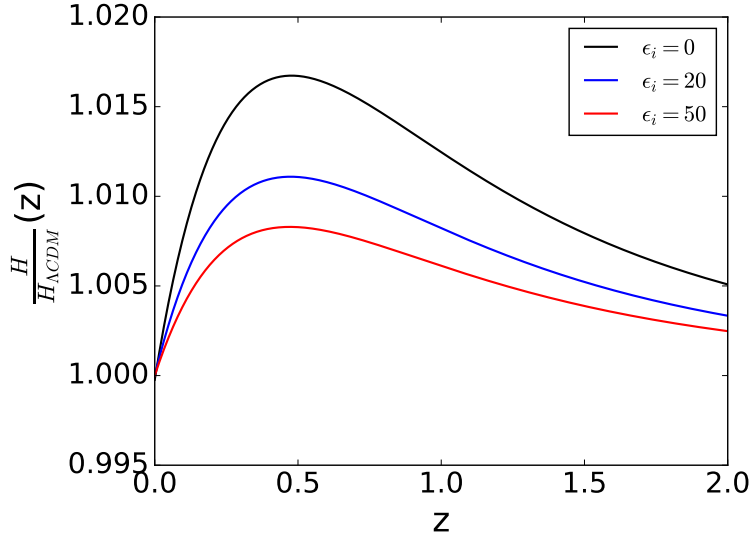


Figure 3. Deviations in the Hubble parameter compared to the Λ CDM model.

higher than the Λ CDM value.

4 Evolution of perturbations

In the quasi-static approximation (on sub-Hubble scale) to the full general relativistic perturbation, the linear evolution of the matter-energy density contrast has the standard form given by [37, 43]

$$\ddot{\delta}_m^{qs} + 2H\dot{\delta}_m^{qs} - 4\pi G_{eff}\bar{\rho}_m\delta_m^{qs} = 0. \quad (4.1)$$

where $G_{eff} = \left(1 + \frac{\beta^2\dot{\phi}^4}{2AM_{pl}^2}\right)G = \left(1 + \frac{x^2\epsilon^2}{12A}\right)G$ with G being the Newtonian gravitational constant and A is given by [37, 43]

$$\begin{aligned} A &= 1 - 2\beta \left(2H\dot{\phi} + \ddot{\phi}\right) - \frac{\beta^2\dot{\phi}^4}{2M_{pl}^2} \\ &= \frac{x(-2(B-4)\epsilon^2 + 8\epsilon + 12) - x^3\epsilon^2(\epsilon + 1) + 2\sqrt{6}\lambda y^2\epsilon}{12x(\epsilon + 1)}, \end{aligned} \quad (4.2)$$

where, $B = 3 + \frac{\dot{H}}{H^2} = 1.5(1 - w_\phi\Omega_\phi)$. The superscript 'qs' to the matter-energy density contrast (δ_m) refers to the fact that the Eq. (4.1) is valid in the quasi-static approximation.

Since there is no coupling between matter and Galileon field, it is expected that $G_{eff} \approx G$. To show that G_{eff} is indeed nearly equal to G , in the left panel of Fig. 4, we have plotted percentage deviation of G_{eff} from G . We can see that the deviations are less than 0.1%. This result proves that in our case, we can simply use the Newtonian perturbation theory to study the perturbation in the sub-Hubble limit. In the Newtonian perturbation theory, the evolution equation of the matter-energy density contrast is given by [83–93]

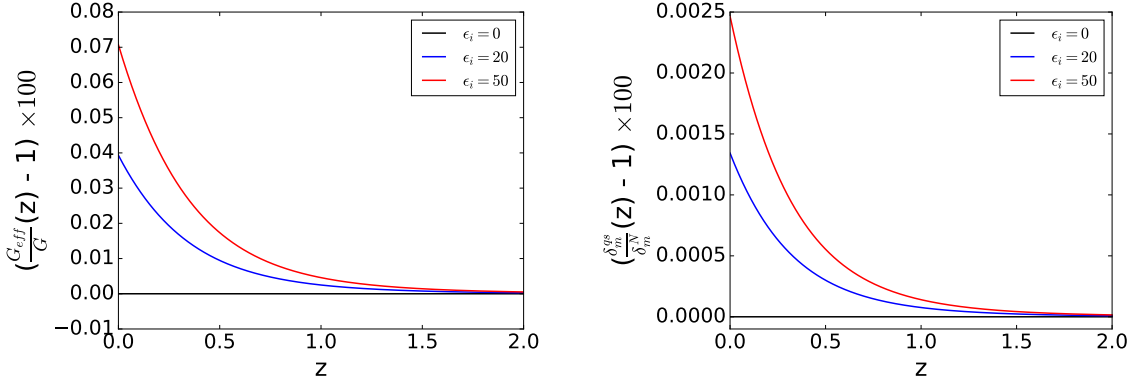


Figure 4. Left panel: Percentage deviation of G_{eff} from G . Right panel: Percentage deviation of δ_m^{qs} from δ_m^N .

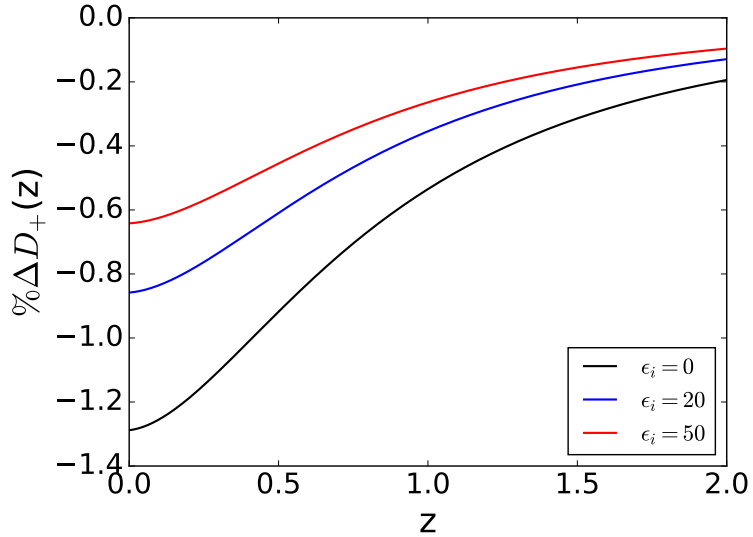


Figure 5. Percentage deviation in growing mode linear growth function from Λ CDM model.

$$\ddot{\delta}_m^N + 2H\dot{\delta}_m^N - 4\pi G\bar{\rho}_m\delta_m^N = 0, \quad (4.3)$$

where the superscript 'N' to the matter-energy density contrast (δ_m) refers to the fact that the Eq. (4.3) is valid in the Newtonian approximation. To solve δ_m^{qs} in Eq. (4.1) or δ_m^N in Eq. (4.3) we consider $\delta_m \propto a$ for both initially at $z = 1100$; i.e. we consider $\delta_m^{qs}|_i = \delta_m^N|_i = \frac{1}{1+1100} = \frac{d\delta_m^{qs}}{dN}|_i = \frac{d\delta_m^N}{dN}|_i$. Note that for both the δ_m we consider growing mode solutions. In the right panel of Fig. 4, we have plotted percentage deviation of δ_m^{qs} from δ_m^N to show again that we can safely take Newtonian perturbation theory in our case. The deviations are less than 0.01%. So, now onwards we shall use the Newtonian perturbation theory on the sub-Hubble scale and for simplicity, we omit the superscript 'N'.

The growing mode solution can be described by a quantity called growth function (D_+) which is defined as $\delta_m(z) = D_+(z)\delta_m^i$. Rewriting Eq. (4.3) with respect to N and using the definition of the growth function we get [85, 93]

$$\frac{d^2 D_+}{dN^2} + \frac{1}{2} \left(1 - 3w_\phi \Omega_\phi\right) \frac{dD_+}{dN} - \frac{3}{2} \Omega_m D_+ = 0 \quad (4.4)$$

To solve the growing mode growth function we use the same initial conditions as in δ_m i.e. $D_+ \propto a$ which gives $D_+|_i = \frac{1}{1+1100} = \frac{dD_+}{dN}|_i$.

In Fig. 5 we have plotted the percentage deviations in the growing mode linear growth function for the cubic Galileon models compared to the Λ CDM model. In this figure and in all the next figures, by the notation '% Δ ' we mean percentage deviation i.e. $\% \Delta Q = \frac{Q_G - Q_{\Lambda CDM}}{Q_{\Lambda CDM}} \times 100$ for any quantity, Q and subscript 'G' corresponds to it's value in the cubic Galileon model. During structure formation, the overdense regions grow with time due to the gravitational attraction between matters. The Galileon field has the negative pressure which produces repulsive gravitational force. The presence of the Galileon field slows down the expansion rate of the overdense regions due to this repulsive gravitational force. For this reason, the model in which Galileon field dominates earlier has the smaller growth rate. That is why in Fig. 5, we can see that the deviations in D_+ for the Galileon models are always negative compared to the Λ CDM model as because cubic Galileon models are always non-phantom. Since in the $\epsilon_i = 0$ model, the Galileon field dominates earliest over matter, the deviations in the D_+ for $\epsilon_i = 0$ model is the largest from the Λ CDM model. Larger the ϵ_i value smaller the deviation. So, the results in Fig. 5 are completely consistent with the results of the Figs. 1, 2 and 3.

4.1 Matter power spectrum

The matter power spectrum, P_m is defined as $\langle \tilde{\delta}_m(\vec{k}, z) \tilde{\delta}_m^*(\vec{k}', z) \rangle = (2\pi)^3 \delta_D^3(\vec{k} - \vec{k}') P_m(k, z)$, where $\tilde{\delta}_m$ is the fourier transform of the δ_m and k is the magnitude of \vec{k} . From this definition we find a relationship between the linear matter power spectrum and initial power spectrum at sufficiently early time given by [83, 85, 93]

$$P_{lin}(k, z) = \frac{D_+^2(z)}{D_+^2(z_{in})} P_{in}(k), \quad (4.5)$$

where, $P_{in}(k) = P_{lin}(k, z_{in})$ is the initial matter power spectrum and for simplicity we have omitted the subscript 'm'. We compute initial matter power spectrum from CAMB [108]. In the CAMB we first compute linear matter power spectrum at redshift $z = 0$ using Λ CDM model for the cosmological parameters given by $\Omega_m^{(0)} = 0.3$, $\Omega_b^{(0)} = 0.05$, $H_0 = 100h km/Sec/Mpc$ with $h = 0.678$, $n_s = 0.968$ and $\sigma_8^{(0)} = \sigma_8(z = 0) = 0.83$. Here, $\Omega_m^{(0)}$, $\Omega_b^{(0)}$ and H_0 are the present day total matter energy density parameter, baryonic matter energy density parameter and Hubble parameter respectively. n_s be the scalar spectral index of the primordial perturbation. $\sigma_8^{(0)}$ is the present day value of the rms fluctuation of mass within the boxes of $8h^{-1}Mpc$ length scale. With these cosmological parameter values in the Λ CDM model the value $\sigma_8^{(0)} = 0.83$ corresponds to the scalar power spectrum amplitude $A_s \simeq 2.27 \times 10^{-9}$ at pivot scale $k_p = 0.05Mpc^{-1}$ related to the primordial curvature perturbation. These values are consistant with the Plank 2015 results [5, 8]. After computing linear matter power spectrum at redshift $z = 0$, we use linear matter growth function for Λ CDM model to compute the matter power spectrum at initial time ($z_{in} = 1100$). We use this initial

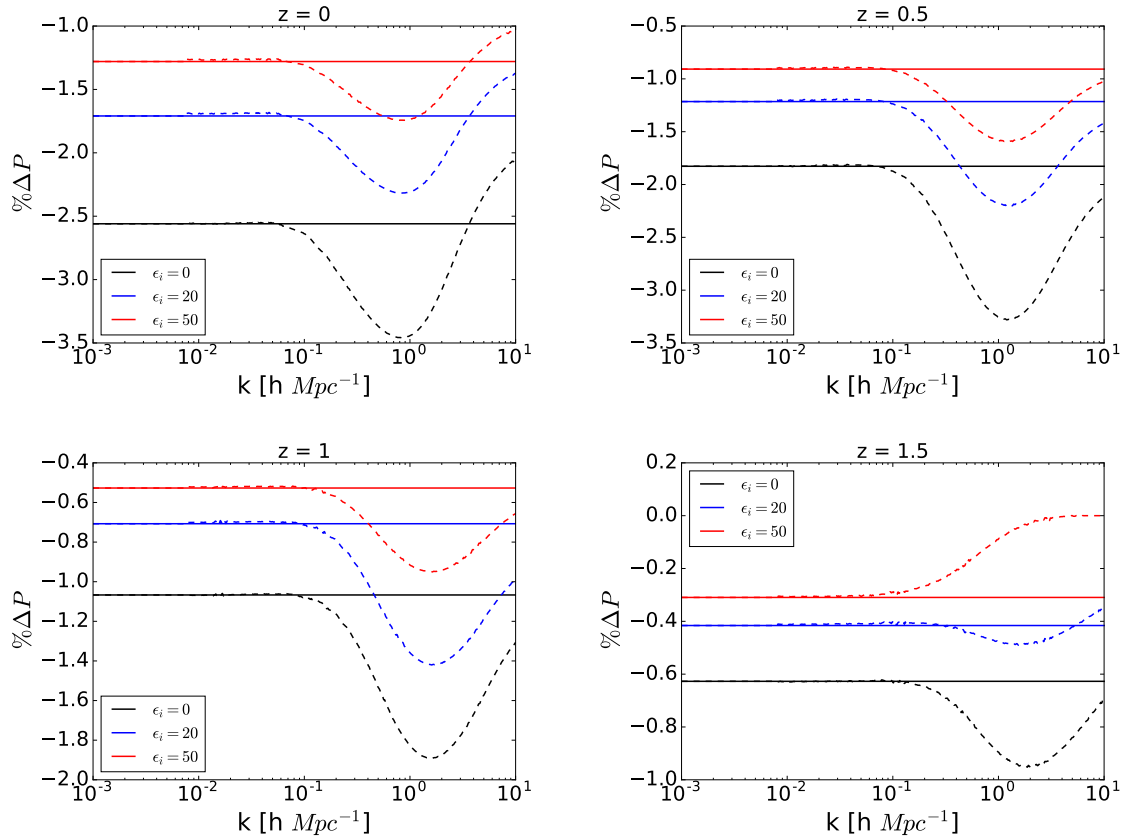


Figure 6. Percentage deviation in the matter power spectrum from the Λ CDM model. Continuous lines are for the linear matter power spectrum described in Eq. (4.5). Dashed lines are for the non-linear matter power spectrum from HMCode [109].

matter power spectrum for all the models i.e. we consider same initial matter power spectrum for all the models.

In Fig. 6, we have plotted percentage deviation in the matter power spectrum for cubic Galileon model with different ϵ_i values compared to the Λ CDM model. The continuous lines are for the deviations in the linear matter power spectrum using Eq. (4.5). The dashed lines correspond to the deviations in the non-linear matter power spectrum. To compute the non-linear matter power spectrum we use HMCode ([109]) for the halofit ppf module in CAMB. The purpose to include the deviations in the non-linear matter power spectrum is that although in the non-linear regime the absolute value of the non-linear matter power spectrum deviates from the linear matter power spectrum, the deviations between two models remains similar (up to a percent only) both in the linear and non-linear matter power spectrum. The deviations in the matter power spectrum are always negative due to the same reason that Cubic Galileon model is always non-phantom irrespective of the value of ϵ_i . The $\epsilon_i = 0$ model has the highest deviation from the Λ CDM model. Larger the value of ϵ_i smaller the deviations. Since linear matter power spectrum is proportional to the square of the linear matter growth functions, the deviations in the linear matter power spectrum are roughly twice the deviations in the linear matter growth functions.

In this figure and in all the next figures dashed lines correspond to the results involving

non-linear matter power spectrum (computed by HMCode) replacing the linear matter power spectrum. The same color corresponds to the same model with continuous and dashed lines correspond to the results using linear and non-linear matter power spectrum respectively.

4.2 Matter bi-spectrum

The matter bi-spectrum, B is defined as $\langle \tilde{\delta}_m(\vec{k}_1, z) \tilde{\delta}_m(\vec{k}_2, z) \tilde{\delta}_m(\vec{k}_3, z) \rangle = (2\pi)^3 \delta_D^3(\vec{k}_1 + \vec{k}_2 + \vec{k}_3) B(\vec{k}_1, \vec{k}_2, \vec{k}_3; z)$. In the Newtonian approximation the tree-level matter bi-spectrum is given by [85, 93]

$$B_{tree}(\vec{k}_1, \vec{k}_2, \vec{k}_3; z) = 2F_2(\vec{k}_1, \vec{k}_2, z)P_{lin}(k_1, z)P_{lin}(k_2, z) + \text{2-cycles}, \quad (4.6)$$

where with the Einstein De-Sitter (EDS) approximation the F_2 is given by [85, 93]

$$F_2(\vec{k}_i, \vec{k}_j) \simeq \frac{5}{7} + \frac{1}{2} \left(\frac{k_i}{k_j} + \frac{k_j}{k_i} \right) \hat{k}_i \cdot \hat{k}_j + \frac{2}{7} (\hat{k}_i \cdot \hat{k}_j)^2, \quad (4.7)$$

Due to the different mode couplings in different triangular shapes, the tree-level matter bi-spectrum is accurate on the scale where $k < 0.1 hMpc^{-1}$. To increase the accuracy of the matter bi-spectrum in weakly non-linear or non-linear regime, we need high precision N-body simulations. However, to get a rough idea about the matter bi-spectrum on non-linear scales, we follow [94] (which is the improved version of [95]). According to [94], the effective matter bi-spectrum which is valid on both linear and non-linear scales given by

$$B_{eff}(\vec{k}_1, \vec{k}_2, \vec{k}_3; z) = 2F_2^{eff}(\vec{k}_1, \vec{k}_2, z)P_{NL}(k_1, z)P_{NL}(k_2, z) + \text{2-cycles}, \quad (4.8)$$

where P_{NL} is the non-linear matter power spectrum and F_2^{eff} is given by [94]

$$\begin{aligned} F_2^{eff}(\vec{k}_i, \vec{k}_j) = & \frac{5}{7} \tilde{a}(n_i, k_i) \tilde{a}(n_j, k_j) + \frac{1}{2} \left(\frac{k_i}{k_j} + \frac{k_j}{k_i} \right) (\hat{k}_i \cdot \hat{k}_j) \tilde{b}(n_i, k_i) \tilde{b}(n_j, k_j) \\ & + \frac{2}{7} (\hat{k}_i \cdot \hat{k}_j)^2 \tilde{c}(n_i, k_i) \tilde{c}(n_j, k_j), \end{aligned} \quad (4.9)$$

where we can see F_2 in Eq. (4.7) gets modified by \tilde{a} , \tilde{b} and \tilde{c} factors which are given by [94]

$$\begin{aligned} \tilde{a}(n, k) &= \frac{1 + \sigma_8^{a_6}(z)[0.7Q_3(n)]^{1/2}(qa_1)^{n+a_2}}{1 + (qa_1)^{n+a_2}} \\ \tilde{b}(n, k) &= \frac{1 + 0.2a_3(n+3)(qa_7)^{n+3+a_8}}{1 + (qa_7)^{n+3.5+a_8}} \\ \tilde{c}(n, k) &= \frac{1 + 4.5a_4/[1.5 + (n+3)^4](qa_5)^{n+3+a_9}}{1 + (qa_5)^{n+3.5+a_9}}, \end{aligned} \quad (4.10)$$

where n is the slope of the linear matter power spectrum at wavenumber k and it is given by [94]

$$n \equiv \frac{d \log P_{lin}(k)}{d \log k}, \quad (4.11)$$

Q_3 , a function of n given by [94]

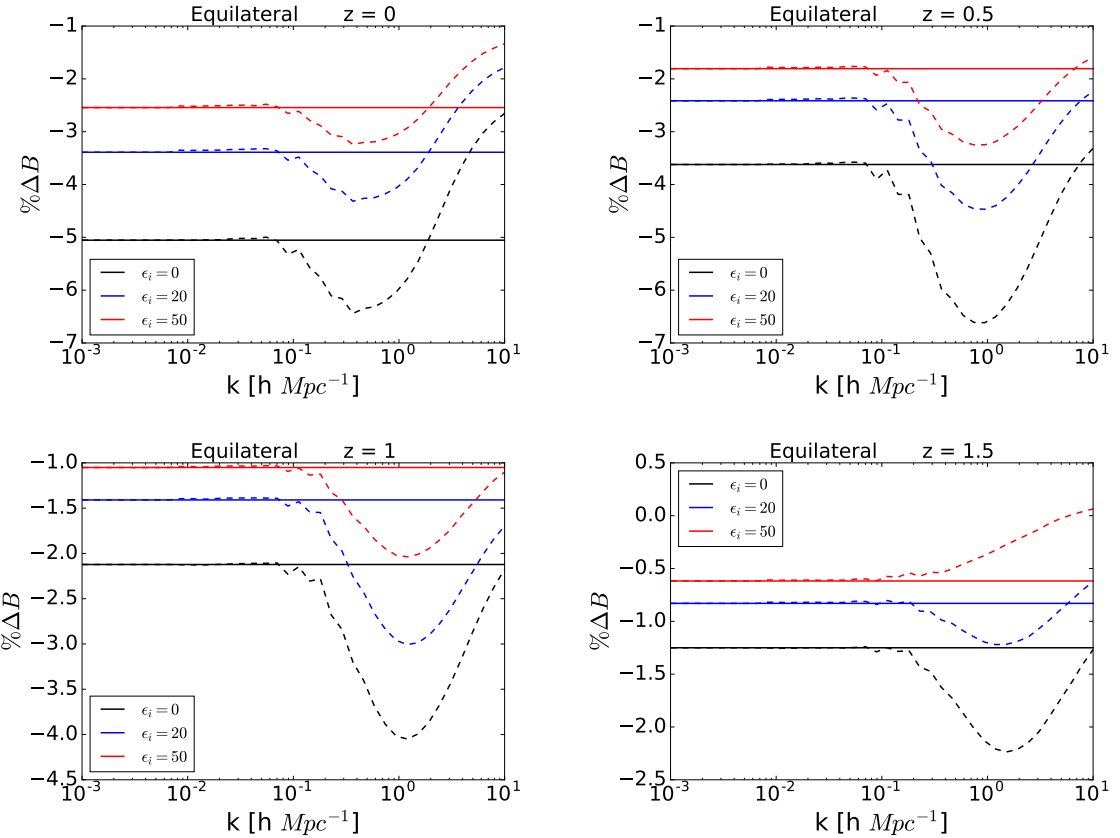


Figure 7. Percentage deviation in the matter bi-spectrum from Λ CDM model for the equilateral configuration. Continuous lines are for the tree-level matter bi-spectrum described in Eq. (4.6). Dashed lines are for the non-linear effective matter bi-spectrum described in Eq. (4.8).

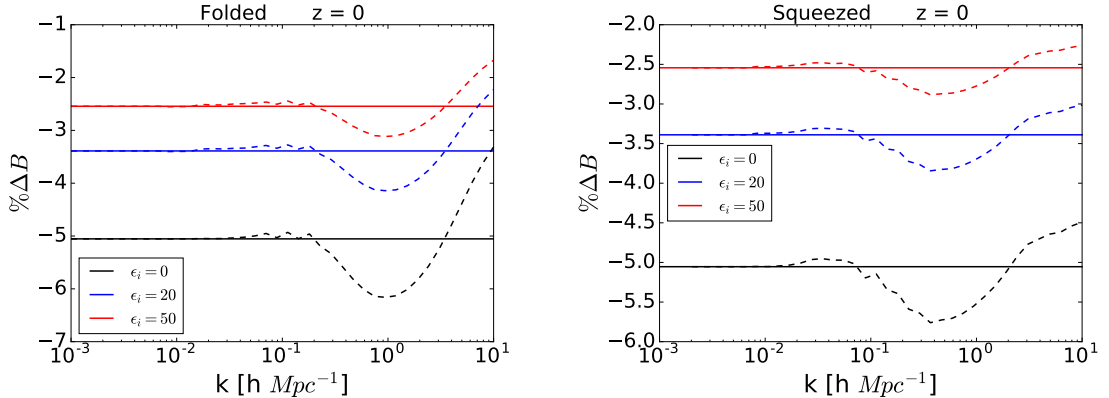


Figure 8. Plots similar to the top-left panel of the Fig. 7 but for the folded (left panel) and squeezed (right panel) configurations respectively.

$$Q_3(n) = \frac{4 - 2^n}{1 + 2^{n+1}}, \quad (4.12)$$

q is defined as $q \equiv k/k_{nl}$, where k_{nl} is the scale up to which linear matter power spectrum is accurate enough and it is computed by [94]

$$\frac{k_{nl}^3 P_{lin}(k_{nl})}{2\pi^2} = 1, \quad (4.13)$$

the σ_8 parameter at a particular redshift given by $\sigma_8(z) = \frac{D_+(z)}{D_+(z=0)} \sigma_8(z=0)$ and finally the constants a_1 to a_9 are given by [94]

$$\begin{aligned} a_1 &= 0.484 & a_2 &= 3.740 & a_3 &= -0.849 \\ a_4 &= 0.392 & a_5 &= 1.013 & a_6 &= -0.575 \\ a_7 &= 0.128 & a_8 &= -0.722 & a_9 &= -0.926 \end{aligned} \quad (4.14)$$

So, the tree-level matter bi-spectrum in Eq. (4.6) gets modified through two ways: one is simply replacing linear matter power spectrum with non-linear matter power spectrum and another is through the modification of F_2 denoted by F_2^{eff} . For more details of the effective matter bi-spectrum, refer to [94].

In Fig. 7 we plot deviations in the matter bi-spectrum for the cubic Galileon models compared to the Λ CDM model for the equilateral configuration ($k_1 = k_2 = k_3 = k$). For a particular color i.e. for a particular model the continuous and dashed lines correspond to the tree-level (using Eq. (4.6)) and effective (using Eq. (4.8)) matter bi-spectrum respectively. we can see that the changes in the deviations for effective matter bi-spectrum from the tree-level matter bi-spectrum is not significant (upto few percentage level). The deviation in the tree-level (or in the effective) matter bi-spectrum is the most for the $\epsilon_i = 0$ model and decreases with increasing ϵ_i . The deviation in the tree-level matter bi-spectrum is roughly twice the deviation in the linear matter power spectrum because B_{tree} contains P_{lin}^2 terms in Eq. (4.6). Here also all the deviations are negative because cubic Galileon models are always non-phantom.

In Fig. 8 we have plotted percentage deviations in the matter bi-spectrum from the Λ CDM model at $z = 0$ similar to the top-left panel of the Fig. 7 but for two other triangular configurations. Left and right panels are for the folded ($k_1 = 2k_2 = 2k_3 = k$) and squeezed ($k_1 = k_2 = 20k_3 = k$) configurations respectively. The results are almost similar in the folded and squeezed configurations compared to the equilateral configuration.

5 Weak lensing statistics

In the context of the structure formation, matter power spectrum or any higher order statistical quantities like matter bi-spectrum, trispectrum etc. are not directly measurable. In literature among the different direct observational aspects, weak lensing statistics is an important application to probe the underlying matter distribution. Weak lensing is one of the strongest probes to the structure formation history of the Universe. Weak gravitational lensing is an intrinsically statistical measurement of the distortion effect of the images of the background galaxies due to the bending of light rays by matter along the line of sight between distant background galaxies and us. This image distortion effect is quantified by an important quantity called convergence. The convergence, κ can probe the underlying matter distribution (δ_m) and it is thus defined as [96–99]

$$\kappa(\hat{n}, \chi) = \int_0^\chi W(\chi') \delta_m(\hat{n}, \chi') d\chi', \quad (5.1)$$

where the integration is along the line of sight with a weight function denoted by $W(\chi)$. \hat{n} is the direction in which we measure the distortion effect and χ is the comoving distance. Note that the above equation is valid in the weak lensing limit and in the Newtonian perturbation theory. The weight function W at a particular comoving distance (or at a particular redshift) is given by [96–99]

$$W(\chi(z)) = \frac{3}{2} \Omega_m^{(0)} H_0^2 g(z)(1+z), \quad (5.2)$$

where g is given by [96–99]

$$g(z) = \chi(z) \int_z^\infty dz' n(z') \left(1 - \frac{\chi(z')}{\chi(z)}\right), \quad (5.3)$$

In literature $g(z)/\chi(z)$ is called the geometric lensing efficiency factor. Here $n(z)$ is the source distribution function. It is normalized by the condition $\int_0^\infty n(z) dz = 1$. We consider a particular source distribution given by [93, 96–99]

$$n(z) = \frac{\left(\frac{1+b_1}{z_0}\right)}{\Gamma\left(\frac{1+b_1+b_2}{b_2}\right)} \left(\frac{z}{z_0}\right)^{b_1} \exp\left[-\left(\frac{z}{z_0}\right)^{b_2}\right], \quad (5.4)$$

where the normalization condition $\int_0^\infty n(z) dz = 1$ has been used. And we consider $b_1 = 2$, $b_2 = 1.5$ and $z_0 = 0.9/1.412$ which are similar to the Euclid Survey [104–107].

5.1 Convergence power spectrum

The convergence power spectrum, P_κ is defined as (assuming statistical isotropy)

$$\langle \kappa_{lm} \kappa_{l'm'}^* \rangle = \delta_{ll'} \delta_{mm'} P_\kappa(l), \quad (5.5)$$

where κ_{lm} is the fourier transform of $\kappa(\hat{n}, \chi)$ in the multipole (l, m) space and it is given by

$$\kappa_{lm} = \int d\hat{n} \kappa(\hat{n}, \chi) Y_{lm}^*, \quad (5.6)$$

where Y_{lm} are the spherical harmonics. In the Newtonian perturbation theory and using the Limber approximation the convergence power spectrum becomes [96–101]

$$P_\kappa(l) = \int_0^\infty \frac{dz}{H(z)} \frac{W^2(\chi(z))}{\chi^2(z)} P\left(\frac{l}{\chi(z)}, z\right). \quad (5.7)$$

In Fig. 9 we have plotted percentage deviations in the convergence power spectrum for the cubic Galileon models from the Λ CDM model. The same color corresponds to the same value of ϵ_i whereas continuous and dashed lines correspond to the computation of the convergence power spectrum by using linear and non-linear power spectrum respectively in Eq. (5.7). As because cubic Galileon models are always non-phantom, the deviations here are always negative similar to the previous results. The deviation is the largest for the $\epsilon_i = 0$ model. The deviation decreases with increasing ϵ_i . Note that the deviations increase with increasing l . This is because of the fact that different dark energy models have different

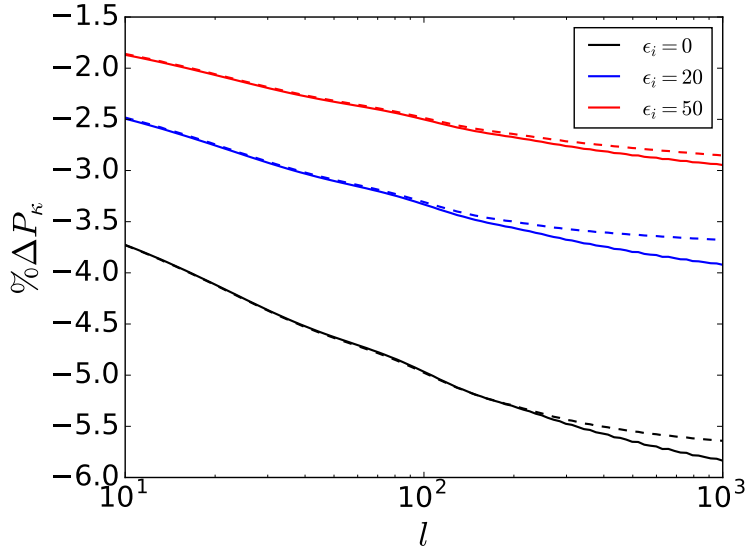


Figure 9. Percentage deviation in convergence power spectrum from the Λ CDM model. Continuous lines are for the results putting linear matter power spectrum of Eq. (4.5) into Eq. (5.7). Dashed lines are for the results putting the non-linear matter power spectrum from HMCode [109] into Eq. (5.7).

comoving distance at a fixed redshift. So, in the argument of the power spectrum same \mathbf{k} corresponds to the different l at a particular redshift for different dark energy models. For this reason, the scale dependency arises in the deviations in the convergence power spectrum although there is no scale dependency in the deviations in the matter power spectrum. Now, smaller comoving distance corresponds to lesser the intervening matter components and hence lesser the intervening matter energy density. Hence weak lensing signal reduces. Since cubic Galileon model is always non-phantom the weak lensing signal is less in this model compared to the Λ CDM model. So, the deviations in the convergence power spectrum increase in the negative y-axis with increasing l . We can notice that the deviations between linear and non-linear results are accurate enough (less than a percent) up to a scale $l = 10^3$.

5.2 Convergence bi-spectrum

The convergence bi-spectrum is defined as [96, 98, 102, 103]

$$\langle \kappa_{l_1 m_1} \kappa_{l_2 m_2} \kappa_{l_3 m_3} \rangle = \begin{pmatrix} l_1 & l_2 & l_3 \\ m_1 & m_2 & m_3 \end{pmatrix} B_{l_1 l_2 l_3}^\kappa, \quad (5.8)$$

where $\begin{pmatrix} l_1 & l_2 & l_3 \\ m_1 & m_2 & m_3 \end{pmatrix}$ is the Wigner 3-j symbol. In the above definition $B_{l_1 l_2 l_3}^\kappa$ is the full sky convergence bi-spectrum and it is related to the flat sky convergence bi-spectrum given by [102]

$$B_{l_1 l_2 l_3}^\kappa = \begin{pmatrix} l_1 & l_2 & l_3 \\ 0 & 0 & 0 \end{pmatrix} \sqrt{\frac{(2l_1 + 1)(2l_2 + 1)(2l_3 + 1)}{4\pi}} B_\kappa(\vec{l}_1, \vec{l}_2, \vec{l}_3; z). \quad (5.9)$$

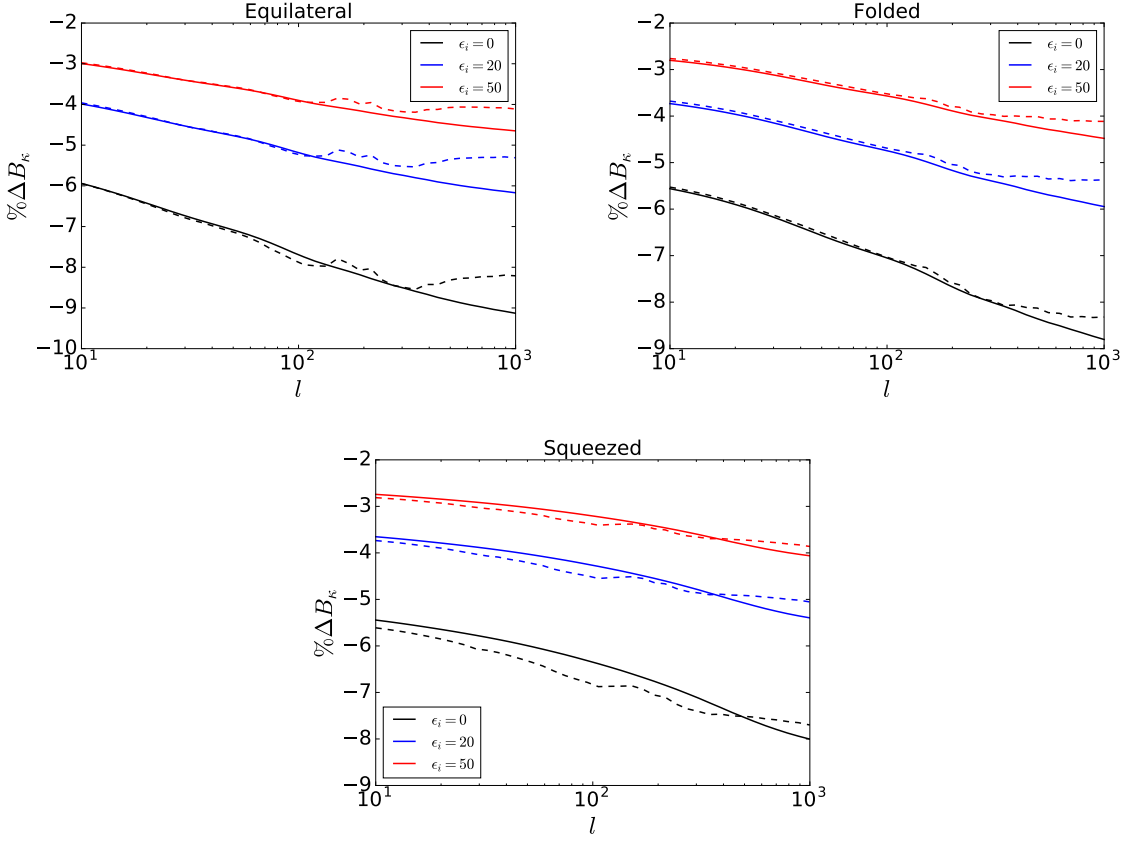


Figure 10. Percentage deviation in convergence bi-spectrum from the Λ CDM model. Continuous lines are for the results putting tree-level matter bi-spectrum of Eq. (4.6) into Eq. (5.10). Dashed lines are for the results putting the effective non-linear matter bi-spectrum of Eq. (4.8) into Eq. (5.10).

In the Newtonian perturbation theory and using the Limber approximation, convergence bi-spectrum becomes [96, 98, 102, 103]

$$B_\kappa(\vec{l}_1, \vec{l}_2, \vec{l}_3; z) = \int_0^\infty \frac{dz}{H(z)} \frac{W^3(\chi(z))}{\chi^4(z)} B\left(\frac{\vec{l}_1}{\chi(z)}, \frac{\vec{l}_2}{\chi(z)}, \frac{\vec{l}_3}{\chi(z)}; z\right), \quad (5.10)$$

with $\vec{l}_1 + \vec{l}_2 + \vec{l}_3 = 0$.

In Fig. 10 percentage deviations in the convergence bi-spectrum from the Λ CDM model has been plotted using equation (5.10) for the equilateral ($l_1 = l_2 = l_3 = l$), folded ($l_1 = 2l_2 = 2l_3 = l$) and squeezed ($l_1 = l_2 = 20l_3 = l$) configurations respectively. First of all note that since we have compared the results between two dark energy models, the results are exactly same for both the flat sky and full sky convergence bi-spectrum. The same color corresponds to the same value of ϵ_i . The continuous lines correspond to the results of using the tree-level matter bi-spectrum of Eq. (4.6) in Eq. (5.10). The dashed lines correspond to the results of using the effective non-linear matter bi-spectrum of Eq. (4.8) in Eq. (5.10). The results are almost similar in the three configurations. Since the cubic Galileon models are always non-phantom, the deviations are always negative as consistent to the previous results. The deviations in the convergence bi-spectrum increase with increasing l because

of the same reason mentioned before (in the discussion of the deviations in the convergence power spectrum). The deviation is the most for $\epsilon_i = 0$ and decreases with increasing ϵ_i . Here also we can see that the linear and non-linear results are less than percentage level up to $l = 10^3$ scale.

6 Conclusion

We have considered lowest non-trivial order action of the full Galileon action i.e. the cubic Galileon model to study the late-time cosmic acceleration. We have studied the signature of the cubic Galileon model on the growth of the structures through the convergence power spectrum and bi-spectrum.

The deviations in the convergence power spectrum are 2.5 to 5% at $l = 10^2$ for the cubic Galileon models from the Λ CDM model. The deviations increase with increasing l . To compute the convergence power spectrum we have considered both the linear and non-linear matter power spectrum and the differences in the results are less than 1% up to $l = 10^3$. The linear results are very accurate up to the scale $l \approx 10^2$.

The deviations in the convergence bi-spectrum are 4 to 8% at $l = 10^2$ for the cubic Galileon models from the Λ CDM model for the equilateral configuration. The results are almost similar for the folded and squeezed configurations. The deviations increase with increasing l . To compute the convergence bi-spectrum we have considered both the tree-level and the effective non-linear matter bi-spectrum and the differences in the two results are sub-percentage up to the scale $l = 10^3$.

In summary, future high precision cosmological observations like DES, LSST, Euclid, WFIRST etc. can decisively detect the cubic Galileon models from the Λ CDM model or from the quintessence models through the measurements of the convergence power spectrum and bi-spectrum.

Acknowledgments

The author would like to acknowledge Council of Scientific & Industrial Research (CSIR), Govt. of India for financial support through Senior Research Fellowship (SRF) scheme No:09/466(0157)/2012-EMR-I.

References

- [1] A. G. Riess et al. (Supernova Search Team), *Astron. J.* 116, 1009 (1998), [astro-ph/9805201](#).
- [2] S. Perlmutter et al. (Supernova Cosmology Project), *Astrophys. J.* 517, 565 (1999), [astro-ph/9812133](#).
- [3] D. N. Spergel et al. (WMAP), *Astrophys. J. Suppl.* 148, 175 (2003), [astro-ph/0302209](#).
- [4] G. Hinshaw et al. (WMAP), *Astrophys. J. Suppl.* 148, 135 (2003), [astro-ph/0302217](#).
- [5] Ade P. A. R., et al., *A&A* 594, A13 (2016), preprint [[arxiv: astro-ph/1502.01589](#)].
- [6] T. Delubac, J. E. Bautista, N. G. Busca, J. Rich, D. Kirkby, S. Bailey, A. Font-Ribera, A. Slosar, K.-G. Lee, M. M. Pieri, et al., *Astron. Astrophys.* 574, A59 (2015), [1404.1801](#).
- [7] M. Ata et al. (2017), [1705.06373](#).
- [8] Ade P. A. R., et al., *A&A* 594, A20 (2016), preprint [[arxiv: astro-ph/1502.02114](#)].
- [9] Sahni V., Starobinsky A., 2000, *International Journal of Modern Physics D*, 9, 373.

- [10] Sahni V., Shafieloo A., Starobinsky A. A., 2014, *ApJ*, 793, L40.
- [11] Delubac T., et al., 2015, *A&A*, 574, A59.
- [12] Riess A. G., et al., 2016, preprint [arxiv: astro-ph/1604.01424].
- [13] Bonvin V., et al., 2016, preprint [arxiv: astro-ph/1607.01790].
- [14] I. Zlatev, L. M. Wang and P. J. Steinhardt, *Phys. Rev. Lett.* 82, 896 (1999) [arXiv:astro-ph/9807002].
- [15] P. J. Steinhardt, L. M. Wang and I. Zlatev, *Phys. Rev. D* 59, 123504 (1999) [arXiv:astro-ph/9812313].
- [16] Caldwell R. R., Linder E. V., 2005, *Phys. Rev. Lett.*, 95, 141301.
- [17] Eric V. Linder, *Phys. Rev. D* 73, 063010 (2006).
- [18] Shinji Tsujikawa, "Dark energy: investigation and modeling" [arxiv: 1004.1493].
- [19] Scherrer R. J., Sen A. A., 2008, *Phys. Rev.*, D77, 083515.
- [20] Bikash R. Dinda and Anjan A Sen, "Imprint of thawing scalar fields on large scale galaxy overdensity" [arxiv: 1607.05123].
- [21] T. Chiba, *Phys. Rev. D* 79, 083517 (2009) Erratum: [*Phys. Rev. D* 80, 109902 (2009)] [arXiv:0902.4037 [astro-ph.CO]].
- [22] T. Clifton, P. G. Ferreira, A. Padilla and C. Skordis, *Phys. Rept.* 513, 1 (2012) [arXiv:1106.2476 [astro-ph.CO]].
- [23] K. Hinterbichler, *Rev. Mod. Phys.* 84, 671 (2012) [arXiv:1105.3735 [hep-th]].
- [24] C. de Rham, *Comptes Rendus Physique* 13, 666 (2012) [arXiv:1204.5492 [astro-ph.CO]].
- [25] C. de Rham, *Living Rev. Rel.* 17, 7 (2014) [arXiv:1401.4173 [hep-th]].
- [26] A. De Felice and S. Tsujikawa, *Living Rev. Rel.* 13, 3 (2010) [arXiv:1002.4928 [gr-qc]].
- [27] A. Nicolis, R. Rattazzi and E. Trincherini, The Galileon as a local modification of gravity, *Phys. Rev. D* 79 (2009) 064036 [arXiv:0811.2197] [INSPIRE].
- [28] N. Chow and J. Khoury, *Phys. Rev. D* 80, 024037 (2009) [arXiv:0905.1325 [hep-th]].
- [29] F. P. Silva and K. Koyama, *Phys. Rev. D* 80, 121301 (2009) [arXiv:0909.4538 [astro-ph.CO]].
- [30] T. Kobayashi, *Phys. Rev. D* 81, 103533 (2010) [arXiv:1003.3281 [astro-ph.CO]].
- [31] T. Kobayashi, H. Tashiro and D. Suzuki, *Phys. Rev. D* 81, 063513 (2010) [arXiv:0912.4641 [astro-ph.CO]].
- [32] A. De Felice, S. Mukohyama and S. Tsujikawa, *Phys. Rev. D* 82, 023524 (2010) [arXiv:1006.0281 [astro-ph.CO]].
- [33] C. Deffayet, O. Pujolas, I. Sawicki and A. Vikman, *JCAP* 1010, 026 (2010) [arXiv:1008.0048 [hep-th]].
- [34] C. de Rham, G. Gabadadze, L. Heisenberg and D. Pirtskhalava, *Phys. Rev. D* 83, 103516 (2011) [arXiv:1010.1780 [hep-th]].
- [35] C. de Rham and L. Heisenberg, *Phys. Rev. D* 84, 043503 (2011) [arXiv:1106.3312 [hep-th]].
- [36] L. Heisenberg, R. Kimura and K. Yamamoto, *Phys. Rev. D* 89, 103008 (2014) [arXiv:1403.2049 [hep-th]].
- [37] Nicola Bartolo, Emilio Bellini, Daniele Bertacca and Sabino Matarrese, Matter bispectrum in cubic Galileon cosmologies, *JCAP*03(2013)034.
- [38] Emilio Bellini and Raul Jimenez, The parameter space of cubic Galileon models for cosmic acceleration, *Physics of the Dark Universe* 2 (2013) 179–183.

[39] Barreira et. al., Nonlinear structure formation in the cubic Galileon gravity model, JCAP10(2013)027.

[40] Bikash R. Dinda, Md. Wali Hossain and Anjan A Sen, Observed galaxy power spectrum in cubic Galileon model, [arxiv: astro-ph/1706.00567].

[41] Md. Wali Hossain and Anjan A. Sen, Do observations favour Galileon over quintessence?, Physics Letters B 713 (2012) 140–144.

[42] Md. Wali Hossain, First and second order cosmological perturbations in light mass Galileon models, Phys. Rev. D 96, 023506 (2017).

[43] A. Ali, R. Gannouji, M. W. Hossain, and M. Sami, Phys. Lett. B718, 5 (2012), [arxiv:1207.3959].

[44] Barreira et. al., The observational status of Galileon gravity after Planck, JCAP08(2014)059.

[45] C. Deffayet, G. Esposito-FarÃse and A. Vikman, Covariant Galileon, Phys. Rev. D 79, 084003 (2009).

[46] R. Gannouji and M. Sami, Phys. Rev. D82, 024011 (2010), [arxiv:1004.2808].

[47] A. De Felice and S. Tsujikawa, Phys. Rev. Lett. 105, 111301 (2010), [arxiv:1007.2700].

[48] A. Ali, R. Gannouji, and M. Sami, Phys. Rev. D82, 103015 (2010), [arxiv:1008.1588].

[49] D. F. Mota, M. Sandstad, and T. Zlosnik, JHEP 12, 051 (2010), [arxiv:1009.6151].

[50] C. Deffayet, S. Deser, G. Esposito-Farese, Generalized Galileons: All scalar models whose curved background extensions maintain second-order field equations and stress tensors, Phys. Rev. D 80, 064015 (2009), [arxiv:0906.1967].

[51] M. A. Luty, M. Porrati, and R. Rattazzi, JHEP 09, 029 (2003), hep-th/0303116.

[52] G. R. Dvali, G. Gabadadze, and M. Porrati, Phys. Lett. B485, 208 (2000), hep-th/0005016.

[53] R. P. Woodard, Lect. Notes Phys. 720, 403 (2007), astro-ph/0601672.

[54] G. W. Horndeski, Int. J. Theor. Phys. 10, 363 (1974).

[55] C.M. Will, The confrontation between General Relativity and Experiment, Living Rev. Rel. 17 (2014) 4 [arXiv:1403.7377] [IN SPIRE].

[56] A. I. Vainshtein, Phys. Lett. B39, 393 (1972).

[57] H. van Dam and M. J. G. Veltman, Nucl. Phys. B22, 397 (1970).

[58] V. I. Zakharov, JETP Lett. 12, 312 (1970), [Pisma Zh. Eksp. Teor. Fiz.12,447(1970)].

[59] M. Fierz and W. Pauli, Proc. Roy. Soc. Lond. A173, 211 (1939).

[60] Tyson, J. A.; Valdes, F.; Jarvis, J. F.; Mills, A. P., Jr. (June 1984). "Galaxy mass distribution from gravitational light deflection". *Astrophysical Journal*. 281: L59âSL62.

[61] Brainerd, T. G., Blandford, R. D., and Smail, I. 1996, ApJ, 466, 623.

[62] Bacon D. J., Refregier A. R., Ellis R. S., 2000, MNRAS, 318, 625.

[63] Kaiser N., Wilson, G. Luppino G. A., 2000, [arxiv: astro-ph/0003338].

[64] Van Waerbeke L., Mellier Y., Erben T., et al., 2000, A&A, 358, 30.

[65] Wittman D. M., Tyson J. A., Kirkman D., DellâŽAntonio I., Bernstein G., 2000, Nature, 405, 143.

[66] <http://www.darkenergysurvey.org/>.

[67] <http://www.lsst.org/>.

[68] <http://www.euclid-ec.org/>.

[69] R. Massey, J. Rhodes, R. Ellis, N. Scoville, A. Leauthaud et al., *Nature (London)* **445**, 286 (2007).

[70] R. Massey, J. Rhodes, A. Leauthaud, P. Capak, R. Ellis et al., *Astrophys. J. Suppl. Ser.* **172**, 239 (2007).

[71] L. Fu, E. Semboloni, H. Hoekstra, M. Kilbinger, L. van Waerbeke et al., *Astron. Astrophys.* **479**, 9 (2008).

[72] M. Kilbinger, K. Benabed, J. Guy, P. Astier, I. Tereno et al., *Astron. Astrophys.* **497**, 677 (2009).

[73] David J. Bacon, Alexandre R. Refregier and Richard S. Ellis, "Detection of Weak Gravitational Lensing by Large-scale Structure", *Mon. Not. R. Astron. Soc.* **318**, 625 (2000) [arXiv: astro-ph/0003008].

[74] Sirichai Chongchitnan and Lindsay King, "Imprints of dynamical dark energy on weak-lensing measurements", *Mon. Not. R. Astron. Soc.* **407**, 1989â€¢1997 (2010).

[75] T. Schrabback, J. Hartlap, B. Joachimi, M. Kilbinger, P. Simon et al., *Astron. Astrophys.* **516**, A63 (2010).

[76] M. Takada and B. Jain, *Mon. Not. R. Astron. Soc.* **348**, 897 (2004).

[77] H. Hoekstra and B. Jain, *Annu. Rev. Nucl. Part. Sci.* **58**, 99 (2008).

[78] R. Massey, T. Kitching, and J. Richard, *Rep. Prog. Phys.* **73**, 086901 (2010).

[79] Kaiser N., 1992, *ApJ*, **388**, 272.

[80] Jain B., Seljak U., 1997, *ApJ*, **484**, 560

[81] Kamionkoski M., Babul A. Cress C. M., Refregier A., 1997, *MNRAS*, **301**, 1064, [arxiv: astro-ph/9712030].

[82] Wayne Hu and Max Tegmark, *The Astrophysical Journal*, **514**:L65â€¢L68, 1999 April 1 [arxiv: astro-ph/9811168].

[83] Christian Knobel, *An Introduction into the Theory of Cosmological Structure Formation* [arXiv:1208.5931].

[84] F. Bernardeau, S. Colombi, E. Gaztanaga and R. Scoccimarro, Large-scale structure of the Universe and cosmological perturbation theory, *Phys. Rept.* **367** (2002) 1 [astro-ph/0112551] [SPIRES].

[85] E. Sefusatti and F. Vernizzi, Cosmological structure formation with clustering quintessence, *JCAP* **03** (2011) 047 [arXiv:1101.1026] [INSPIRE].

[86] M. Crocce and R. Scoccimarro, Renormalized cosmological perturbation theory, *Phys. Rev. D* **73** 063519, [astro-ph/0509418].

[87] Matteo Fasiello and Zvonimir Vlah, *Phys. Rev. D* **94**, 063516 (2016), preprint [arxiv: astro-ph/1604.04612].

[88] G.Dâ€ŽAmico and E. Sefusatti, *JCAP*, **1111**, 013 (2011).

[89] S. Matarrese and A. Pietroni, Resumming Cosmic Perturbations, *JCAP*, **0706**, 026 (2007) [astro-ph/0703563].

[90] S. Anselmi, S. Matarrese and M. Pietroni, Next-to-leading resummations in cosmological perturbation theory, *JCAP*, **1106**, 015 (2011), arXiv:1011.4477 [astro-ph.CO].

[91] S. Anselmi and M. Pietroni, Nonlinear power spectrum from resummed perturbation theory: a leap beyond the BAO scale, *Journal of Cosmology and Astro-Particle Physics* **12** 13, [arXiv:1205.2235].

- [92] Nonlinear effects of dark energy clustering beyond the acoustic scales JCAP 07 013 (2014) [arXiv:astro-ph/1402.4269].
- [93] Bikash R. Dinda, Probing dark energy using convergence power spectrum and bi-spectrum, JCAP09(2017)035 [arXiv:1705.00657].
- [94] He'ctor Gil-Marin' et al., An improved fitting formula for the dark matter bispectrum, JCAP 02 (2012) 047 [arXiv:astro-ph/1111.4477].
- [95] Scoccimarro, R., & Couchman, H. M. P. 2001, MNRAS, 325, 1312.
- [96] Masanori Sato and Takahiro Nishimichi, Impact of the non-Gaussian covariance of the weak lensing power spectrum and bispectrum on cosmological parameter estimation [arXiv:1301.3588].
- [97] Dragan Huterer, Weak lensing, dark matter and dark energy, Gen Relativ Gravit (2010) 42:2177–2195 [arXiv:1001.1758].
- [98] Masahiro Takada and Bhuvnesh Jain, Cosmological parameters from lensing power spectrum and bispectrum tomography [arXiv:astro-ph/0310125].
- [99] Toshiya Namikawa, CMB Lensing Bispectrum from Nonlinear Growth of the Large Scale Structure [arXiv:1604.08578].
- [100] Mustapha Ishak, Probing decisive answers to dark energy questions from cosmic complementarity and lensing tomography, Mon. Not. R. Astron. Soc. (2005) 363 (2): 469–478, [arXiv:astro-ph/0501594].
- [101] Amol Upadhye, Mustapha Ishak and Paul J. Steinhardt, Dynamical dark energy: Current constraints and forecasts, Phys. Rev. D 72, 063501 (2005), [arXiv:astro-ph/0411803].
- [102] Asantha Cooray And Wayne Hu, WEAK GRAVITATIONAL LENSING BISPECTRUM, The Astrophysical Journal, 548:7–18 2001 February 10 [arXiv:astro-ph/0004151].
- [103] Patrick Valageas, Masanori Sato and Takahiro Nishimichi, Modeling of weak lensing statistics. I. Power spectrum and bispectrum, Astron. Astrophys. (2012), 541, A161 [arXiv:1111.7156].
- [104] Luca et. al., "Cosmology and Fundamental Physics with the Euclid Satellite" Living Rev. Relativity, 16, (2013), 6 [<http://www.livingreviews.org/lrr-2013-6>].
- [105] The Euclid Collaboration 2011, [arXiv: astro-ph/1110.3193].
- [106] Laura Marian, Robert E. Smith, Stefan Hilbert, Peter Schneider, "Optimized detection of shear peaks in weak lensing maps" [arXiv:astro-ph/1110.4635].
- [107] R. Ali Vanderveld, Michael J. Mortonson, Wayne Hu and Tim Eifler, Testing dark energy paradigms with weak gravitational lensing, Phys. Rev. D 85, 103518 (2012).
- [108] A. Lewis, A. Challinor and A. Lasenby, Astrophys. J. 538, 473 (2000); see <http://camb.info/>.
- [109] A. Mead, C. Heymans, L. Lombriser, J. Peacock, O. Steele, and H. Winther, Mon. Not. Roy. Astron. Soc. 459, 1468 (2016); [arXiv: astro-ph/1110.3193].